

Postprint: Kamp, J. & Kraume, M.: Influence of drop size and superimposed mass transfer on coalescence in liquid/liquid dispersions - Test cell design for single drop investigations, *Chem. Eng. Res. Des.*, Elsevier, 2014, 92, 635-643 <http://dx.doi.org/10.1016/j.cherd.2013.12.023>

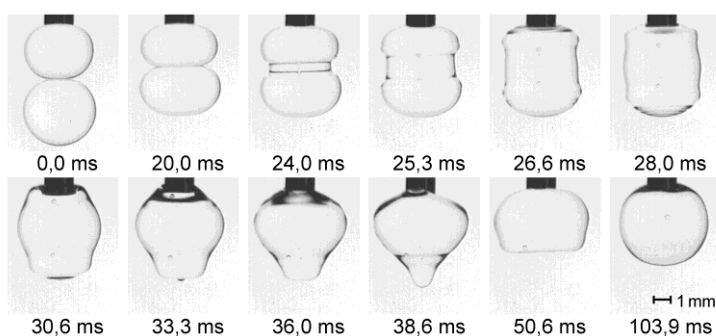
Influence of drop size and superimposed mass transfer on coalescence in liquid/liquid dispersions - Test cell design for single drop investigations

Johannes Kamp^{a*}, Matthias Kraume^a

^a Chair of Chemical & Process Engineering, Technische Universität Berlin, FH 6-1, Fraunhoferstr. 33-36, 10587 Berlin

* Corresponding author, e-mail: johannes.kamp@tu-berlin.de, phone: +49 30 314 23171

The detailed understanding of droplet coalescence is important for the accurate description of liquid/liquid dispersions. A test cell is designed which enables serial examinations of the random coalescence process with high repetition rate, good observability and accuracy of experimental parameters. Within this rectangular test cell a rising droplet collides with a pendant one, while recorded by a high speed camera. The gained experimental data allows a validation and further development of appropriate models. The investigated parameters in this work are the drop size and the superimposed mass transfer influencing the coalescence probability. These examinations were carried out in the EFCE standard test system toluene / acetone / water. The effect of varying the drop size seems to be interfered by the different rising velocities due to buoyancy. Introducing a transferring component has a significant impact on the coalescence process. A transfer direction from disperse to continuous phase results in a coalescence probability of almost 100%, whereas the reverse mass transfer direction induces a repulsion of nearly all droplets.



Keywords

coalescence; test cell; single drop; mass transfer; drop size; coalescence probability

Introduction

Dispersions of at least two liquids showing a miscibility gap are an integral part of several unit operations. Therefore, a detailed understanding and quantitative description of the characteristics and conditions of these systems is important for various technical applications. The most important characteristic of an emulsion is the drop size distribution which affects e.g. the interfacial area and settling time. The drop size distribution is determined by the phenomena breakage and coalescence of single droplets. Thus, these interactions determine the macroscopic behaviour of an emulsion directly. Although various models are available in literature for both phenomena (Liao and Lucas, 2010, 2009), the prediction of the drop size distribution is only possible with restrictions when varying for example the power input or material and process conditions. Consequently, excessive and expensive experimental investigations are still necessary at different scales for process development. For instance, the design of extraction columns still requires pilot plants using high amounts of the original physical system. To diminish the number of influencing factors of the whole process, it is necessary to reduce the problem to the fundamental behaviour of single droplets.

Therefore, the impact of influencing parameters for drop coalescence and breakup needs to be identified and quantified for each phenomenon separately. The gained knowledge of this behaviour can be used to validate existing models or to develop new ones. A modelling approach which accounts for the droplet interactions is the population balance equation, which describes the time dependent drop size distribution by death and birth terms for drop breakage and coalescence (Hulburt and Katz, 1964; Kopriwa et al., 2012; Ramkrishna, 2000, 1985; Randolph and Larson, 1962).

In comparison to the breakage of droplets, Chesters (1991) considers the binary coalescence of two drops as a more complex problem because the interaction of two usually unequally sized droplets has to be considered additionally to the outer continuous phase flow.

In principle droplets have to come into contact, which however does not necessarily result in coalescence, but also in a possible repulsion of the droplets. For an appropriate modelling, the understanding of the coalescence process itself is important, which is divided into several phases (Marrucci, 1969). First of all, the two droplets have to approach each other with a certain relative velocity. Due to fluid dynamic forces the drops are deformed and a thin film of continuous phase is formed between the two drop interfaces. The shape of the film is not planar but lenticular (the so called dimple) so that the outer boundary of the film forms a circular region where the interfaces of the two drops are closer than in the rest of the film (Klaseboer et al., 2000; Mackay and Mason, 1963). For coalescence to occur, the film has to drain until a critical film thickness is reached at which the drop interfaces confluence spontaneously at a certain point. Here, a so called coalescence bridge between the drops is built (Chen et al., 2004; Radoev et al., 1983; Scheludko et al., 1965; Vrij, 1966). From this 'hole' in the film the coalescence front extends rapidly across the contact area driven by the interfacial tension and coalescence of the two droplets occurs (Aarts et al., 2005; Zdravkov et al., 2006). According to these phases of the coalescence process, the crucial influencing factors are the contact time of the droplets, the drainage time of the film, the critical film thickness and the time of confluence. These again depend on the drop properties (e.g. drop sizes, relative velocity), the properties of the phases (e.g. viscosity, density, interfacial tension, surfactants) and the system conditions (e.g. energy dissipation, flow pattern, geometry).

To determine and quantify the influence of these properties, substantial research has been done up to now. However, a broad variety of results can be found in literature which may be caused by the huge amount of influencing parameters. Additionally, the experimental investigation of the coalescence process is a challenging task due to the required high spatial and temporal resolution. Furthermore, a high purity of the fluids is mandatory, as already minor impurities may have a significant impact on the properties of the interface and consequently on the coalescence process (Soika and Pfennig, 2005; Wegener et al., 2009). Published values for the critical film rupture thickness differ from tens (Radoev et al., 1983; Vrij, 1966) to hundreds of nanometres (Zdravkov et al., 2003) although theoretical examination predicts a range of around 1 nanometre (Chesters, 1991; Vrij, 1966). The time span of confluence of the two droplets (or film rupture time) varies from hundreds of microseconds to milliseconds (Aryafar and Kavehpour, 2006; Thoroddsen et al., 2005) whereas the drainage time (or contact time) of the film between two interfaces, which has to elapse for coalescence to occur, has a broad distribution from milliseconds (Sagert and Quinn, 1978; Scheele and Leng, 1971) over seconds (Vijayan and Ponter, 1975) to infinity for stable emulsions (Carroll, 1976).

Most of this theoretical and experimental research has been done for single droplets coalescing with a planar surface (e.g. Aryafar and Kavehpour, 2006; Basheva et al., 1999; Bozzano and Dente, 2011; Charles and Mason, 1960; Dickinson et al., 1988; Hartland, 1967a, 1967b, 1967c; Hool et al., 1998; Jeffreys and Hawksley, 1965; Kourio et al., 1994; Mackay and Mason, 1963; Mohamed-Kassim and Longmire, 2004; Ortiz-Duenas et al., 2010; Thoroddsen, 2006). Extensive theoretical research

has been made modelling the film formation and drainage of two coalescing droplets (e.g. Abid and Chesters, 1994; Baldessari and Leal, 2006; Bozzano and Dente, 2011; Chen, 1985; Chesters, 1991; Danov et al., 1993; Eggers et al., 1999; Ivanov et al., 1999; Klaseboer et al., 2000; Lee and Hodgson, 1968; Marrucci, 1969; Toro-Mendoza and Petsev, 2010).

Experimental studies of droplet-droplet coalescence can be classified by the used set-up. Most investigations were conducted with static set-ups where the droplets are fixed on needles (Ban et al., 2000; Borrell and Leal, 2008; Chen and Pu, 2001; Gaitzsch et al., 2011a; Klaseboer et al., 2000; Pu and Chen, 2001; Sagert and Quinn, 1978; Thoroddsen et al., 2005; Wu et al., 2004) or lying on top of or next to each other (Kumar et al., 2006; Neumann, 1963; Ortiz-Duenas et al., 2010; Vohra and Hartland, 1981). This offers the advantage of good observability and adjustability of drop sizes but is hardly comparable with dispersion interactions in a fluid flow.

Set-ups which offer dynamic collisions differ in their flow patterns. Guido and Simeone (1998) introduced two droplets in an artificial shear flow which caused the collision between them. The research group of Leal (Borrell et al., 2004; Leal, 2004; Yang et al., 2001) performed substantial research of two slowly (Reynolds number of 1) colliding drops injected into a two dimensional linear flow produced by four rolling cylinders. Using a counter flow cell, Gaitzsch et al. (2011b) investigated the coalescence of double emulsions during droplet rising. Eckstein and Vogelpohl (1999) and Simon and Bart (2002) performed drop collisions with a droplet swarm in the same set-up. Although the counter flow cell represents the dynamics in reality quite well, the observability due to optical distortion and lateral movement of the drop is poor and the relative velocity between the rising drop and the droplet swarm is restricted. The collision of freely moving droplets in a stagnant continuous phase was examined by Scheele and Leng (1971) and Eiswirth et al. (2012). Although the two set-ups have considerable limitations, they provide a good observability and similarity to a real dynamic collision. The horizontally colliding drops in the work of Scheele and Leng (1971) require a density similar to the continuous phase or a high velocity to minimize a vertical drift due to buoyancy. The droplets in the work of Eiswirth et al. (2012) are produced by a continuous flow of disperse phase and detach from the needles due to buoyancy and inertia forces. Hence, the drop size and velocity in this set-up depend on the needle size and flow rate of the disperse phase and are therefore only variable independently by a modification of the needles. Additionally, the volume which forms the drop, and thus determines the drop size, cannot be quantified exactly. Due to the high temporal resolution, the accurate triggering of the high speed imaging is a challenging task. Scheele and Leng (1971) used an analogous camera with 5000 frames per second (fps) and wasted a 100 feet (~30 m) roll of film per failed record. Although Eiswirth et al. (2012) was not facing this disadvantage with a digital high speed camera, it was a challenge to record the distinct time and place of the coalescence event.

These findings initiated the design of a new test cell for single drop coalescence analysis performing the following characteristics: dynamic investigations with good observability, precise drop size generation and variation without modification of the set-up, change of relative collision velocity and variability of the liquid phase properties. In addition, a high reproducibility of the single drop collisions with high repetition rate at the same time is inevitable to establish a statistically relevant data base to validate and develop coalescence models. This requires an automation of the complete experimental sequence.

The first application of the test cell investigated the impact of the drop sizes and the superimposed mass transfer on droplet coalescence. The influence of the drop size is not consistently described in literature, but the equivalent droplet diameter which is commonly used in coalescence models (Chesters, 1991; Coualoglou and Tavlarides, 1977; Liao and Lucas, 2010) is defined as:

$$d_{eq} = 2 \frac{d_1 \cdot d_2}{d_1 + d_2}.$$

The decrease of the coalescence probability with increasing droplet size and ratio is described e.g. by the film drainage model of Coulaloglou and Tavlarides (1977) following the dependency:

$$\lambda = \exp(-c_1 \cdot d_{eq}^4)$$

where all other influencing factors of this model (inclusive energy dissipation rate) are lumped in the parameter c_1 in this study. A detailed discussion of the influence of drop diameter and energy dissipation rate described by different models can be found in Kopriwa et al. (2012).

The influence of a superimposed mass transfer was studied previously with two fixed droplets (Ban et al., 2000; Chevaillier et al., 2006) and a fixed drop with an approaching planar interface (Gourdon and Casamatta, 1991). All authors identified an acceleration of the film drainage with mass transfer from disperse to continuous phase and an increased drainage time with inverted mass transfer direction in the systems toluene / acetone / water (Ban et al., 2000; Gourdon and Casamatta, 1991) and glycerol / acetone / silicone oil (Chevaillier et al., 2006). Hence, a significant change in the coalescence probability was observed: drops coalesce immediately with a mass transfer direction from disperse to continuous phase and the coalescence is retarded with a mass transfer from continuous to disperse phase (Gourdon and Casamatta, 1991). This significant influence of the transferring component is often described by a change of the film drainage due to Marangoni effects or a variation of the mutual miscibility of disperse and continuous phase due to the presence of the solute (Kopriwa et al., 2012; Tsouris and Tavlarides, 1993).

Materials & methods

The choice of the physical system with the corresponding properties is in general arbitrary, for a better understanding the set-up will be explained assuming a continuous water phase and a lighter disperse oil phase. The designed test cell combines the advantages of static and dynamic set-ups by inducing the collision of a rising with a pendant droplet (see Fig. 1). The upper oil drop pends on a cannula which can be positioned precisely in all three dimensions. This fixed droplet allows the observation of the collision process at a specific position. The rising oil droplet is generated by a cannula at the bottom of the test cell and is released by a short ejection of continuous water phase. It accelerates and rises over a certain length, adjusted by the position of the upper cannula, and collides with the pendant droplet.

The rectangular test cell has an inner volume of 0.5 litres (height x width x depth: 150 mm x 90 mm x 37 mm) with an outlet at the bottom to guarantee an easy exchange of the continuous phase. The frame is manufactured of stainless steel, the side windows of quartz glass and all seals, tubes and fittings in contact with the investigated fluids are made of PTFE. This choice of chemically highly resistant materials is due to the fact that already small impurities can influence the coalescence behaviour significantly. In addition, the test cell is easily accessible for cleaning. The droplets detach from the cannula's rim at a certain maximum drop diameter if the buoyancy force exceeds the adhesive and interfacial forces. To investigate bigger droplets, the cannula diameter has to be enlarged accordingly. In these investigations the upper cannula size (made of stainless steel 1.4301) was 0.8 mm x 0.6 mm (outer x inner diameter) and the lower cannula (made of borosilicate glass) measured 0.5 mm x 0.2 mm. With these cannulas it was possible to generate drop sizes between 1.5 mm and 3.0 mm at the bottom as well as at the top. The cannula distance could be varied from static direct contact up to 100 mm.

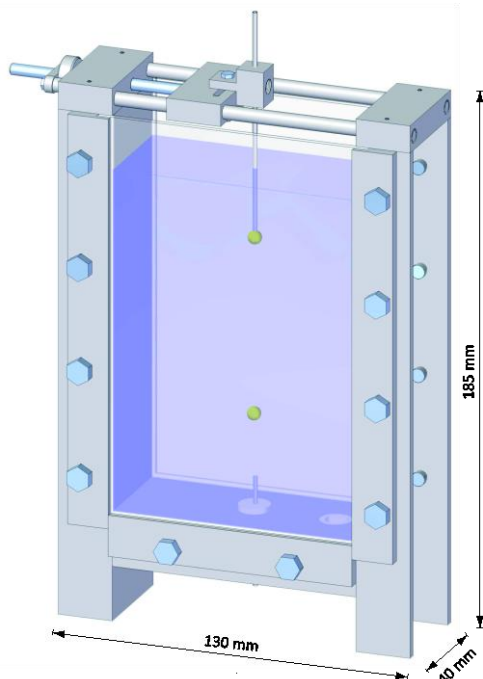


Fig. 1: Side view of the coalescence test cell with rising and pendant droplet

For detailed understanding, the flow diagram of the test cell is shown in Fig. 2. The generation of the droplets is realised by two syringe pumps Hamilton PSD/2 with plug valves. The oil pump (1) has a 3-port valve (Hamilton HVC 3-5) mounted, which is used to distribute the specified oil volumes for the upper and lower droplet. To eject the remaining oil phase to the lower cannula tip and release the droplet afterwards, the water pump (2) with 2-port valve (Hamilton HVC 3-2) is connected to the PTFE tube by a T-fitting (4). This alternating flow of disperse oil and continuous water phase, which is shown schematically in Fig. 2 (4), allows a precise dosing of the droplet volumes, respectively sizes. The used syringes for the present investigations with a volume of 250 μ L (Hamilton TLLX 1725) for the water pump (2) and 50 μ L (Hamilton TLLX 1705) for the oil pump (1) results in a dosing precision of ± 0.125 μ L and ± 0.025 μ L. To detach the sticking drop at the lower cannula, a short pulse of water phase is given by the water pump (2). The intensity and duration of this pulse has to be adjusted carefully preventing an undesired acceleration of the droplet after detachment. Therefore, the volume and velocity of this pulse can be optimized by trial method for every drop size so that the water flow just breaks the link between the cannula's rim and the droplet. The collision of the two drops is recorded by the CMOS high speed camera (5) Photonfocus MV-D752-160-CL-8 (maximum resolution of 752x582 Pixel at a frame rate of 350 fps) with a Pentax TV lens 12 mm mounted and illuminated by the LED flash (6) CCS LDL-TP-100/100-R from the backside of the test cell. After the collision some oil phase may remain at the tip of the upper cannula. Therefore, a second cannula connected to the peristaltic water pump (3) Ismatec IPC 8 is installed sideways to remove these residuals. The temperature inside the test cell is controlled by two U-tube heat exchangers fed by the thermostat (7) Haake D1 and logged by the digital thermometer (8) Greisinger GMH 3710.

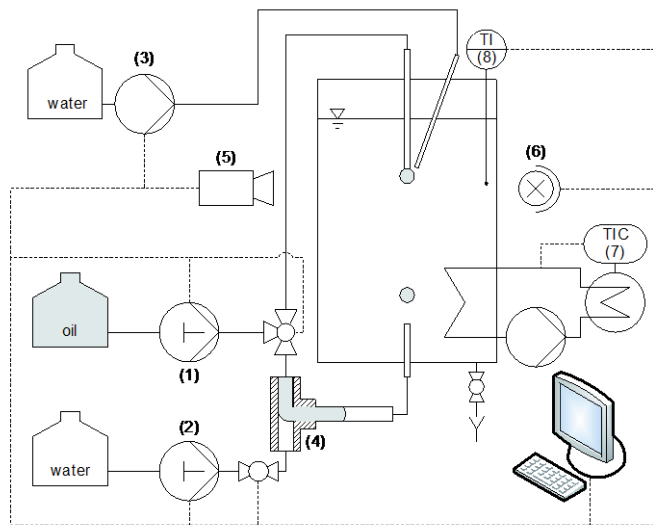


Fig. 2: Flow diagram of the test cell with the components: syringe pumps for (1) oil phase and (2) water phase, (3) peristaltic pump, (4) T-fitting PTFE, (5) high speed camera, (6) LED flash, (7) thermostat, (8) thermometer

The control and automation of the test cell was realised using LabVIEW 2010 from National Instruments. The control routine for the collision of a specified number of droplets n_{drops} is visualised by a structogram in Fig. 3. For each loop a sequence is passed through which initiates a droplet collision recorded by the high speed camera. The focus of this automation was the fast execution of an experimental sequence. Therefore, the image analysis has been moved to a consecutive independent procedure. At the beginning of an experimental sequence the syringe pumps for oil and water are refilled. Then the oil syringe pump generates the upper droplet by ejecting the specified volume V_{up} to the upper cannula. The lower droplet is generated by pumping the specified volume of oil V_{low} via the T-fitting to the lower cannula. Afterwards the remaining oil volume inside the tubes and fittings is filled by the water syringe pump. High speed camera and flash are initialised and the recording begins. Then the lower droplet is detached by a short pulse of water given by the water syringe pump. After the record time for the collision t_{rec} , the camera is stopped and the pictures, the used parameters and the temperature are saved. In the end of a sequence potentially remaining oil phase is removed from the two cannulas by a water jet induced by the peristaltic pump and the water syringe pump.

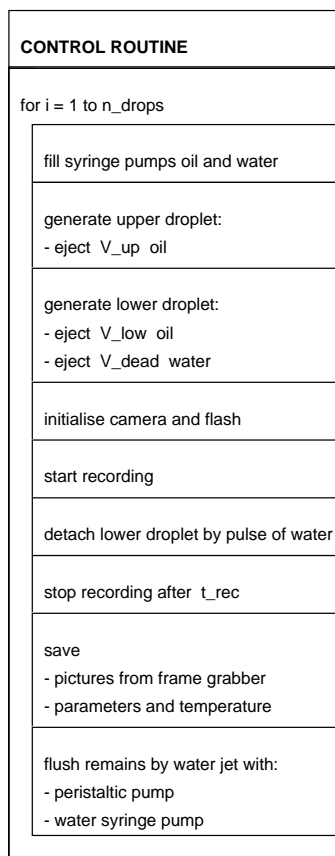


Fig. 3: Structogram for the control routine of the test cell

For the present investigations the EFCE standard test system for extraction (Misek et al., 1985) toluene / acetone / water is used. Accordant to the purity requirements, only chemicals for analysis were used: toluene Merck 1.08325.2500, acetone Merck 1.00014.2500 and ultrapure water with a resistivity of 18.3 M Ω -cm produced by the purification system Werner EASYpure UV. All experiments were conducted at a temperature between 24.0 - 25.0 °C. To avoid undesired mass transfer between toluene and water due to a slight mutual miscibility, the phases were saturated with each other for at least 12 hours before an experiment. Therefore, the phases were prepared in a separatory funnel, which was shaken manually several times, and afterwards separated by settling. Investigating the influence of the transferring component acetone, a certain concentration difference between the two saturated phases was prepared by adding acetone to the disperse or continuous phase, depending on the mass transfer direction. To avoid mass transfer of acetone within the tubes after the T-fitting, the water reservoir of the syringe pump was saturated with acetone accordingly. During the experiments the concentration difference varies due to the accumulation of acetone in the mass receiving phase. This error increases to a deviation of approximately 0.5% in the concentration difference of acetone after 50 droplet collisions of two 3.0 mm drops and mass transfer direction from disperse to continuous phase, which represents the worst case. To avoid a further deviation, the continuous phase was exchanged after 50 droplet collisions.

Results & discussion

The designed test cell for single drop coalescence analysis combines the advantages of static and dynamic set-ups by inducing the collision of a rising with a pendant droplet in a quiescent continuous phase. The immobilization of only one droplet enables dynamic investigations with

good observability. The syringe pumps provide a precise drop size generation and the droplet detachment due to the alternating flow of oil and water phase enables a variation of the drop size without modification of the set-up. Moreover, a change of relative collision velocity and a variation of the liquid phase properties is possible. Due to the automated control sequence 2 - 3 droplet collisions per minute can be recorded by the designed test cell. As presented in Fig. 4 and the appended video, that both show ten recorded sequences merged in parallel, the dosing of the droplet volumes is precise and the collisions are highly reproducible. Hence, the experiments showed that this set-up offers the possibility of serial examinations of the coalescence process under the systematic variation of influencing parameters.

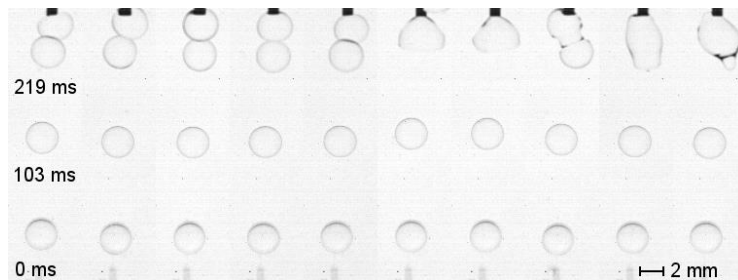


Fig. 4: Video of ten sequences in parallel of a droplet collision ($d_{up} = 2.5$ mm, $d_{low} = 2.5$ mm, cannula distance = 20 mm, 180 frames recorded with 620 fps)

The acting forces are assumed to be mechanically similar to the ones interacting on two freely colliding drops with the same relative velocity, although the same magnitude of relative velocity may act in a different way in different flow fields. In this set-up the relative velocity can be adjusted directly which offers a straightforward validation of the corresponding model assumptions, where the relative velocity is commonly substituted by the energy dissipation rate. Although the quiescent fluid and a fixed droplet are simplifications to the real two phase flow, compared to static experiments the impact of additional dynamic parameters like relative velocity, collision angle and contact time can be investigated. Moreover, the achieved good observability is obligatory for serial examinations and a subsequent quantification of these dynamic parameters.

For each parameter set at least 100 droplet collisions were recorded and analysed to obtain statistically relevant results. In Fig. 5 the trend of the coalescence probability is shown exemplarily over the analysed sequences for equal drop sizes of 2.5 mm and a cannula distance of 20 mm. After 80 sequences the total coalescence probability levels off at $44\% \pm 2\%$. This trend can be detected as well if the angle of collision θ between the droplets' centre of mass is considered. This allows the differentiation between head-on ($\theta = 0^\circ$), slightly off-centre ($\theta < 45^\circ$) and highly eccentric ($\theta > 45^\circ$) collisions, which occur by inevitable small deviations in the rising trajectory of the lower droplets. The total coalescence probability equals the probability of two frontally colliding drops. Corresponding to the analogy between head-on and glancing collision revealed by Borrell et al. (2004), the influence of an eccentric collision is small: the coalescence probability differs by $\pm 5\%$ resulting in a decreased probability of 40% for slightly off-centre collisions and a higher coalescence probability of 50% for highly eccentric contacts. Failed droplet collisions within a sequence (due to incorrect droplet detachment, non-collision, air entrainment, mistaken recording time, etc.) are indicated by skipped symbols in the total coalescence probability of Fig. 5. In this case 53 errors occurred mainly in the last half of the experiment, which is a relatively high number compared to other runs and caused by non-ideal detachment parameters. Nevertheless, these recorded sequences yield a number of 110 analysed droplet collisions.

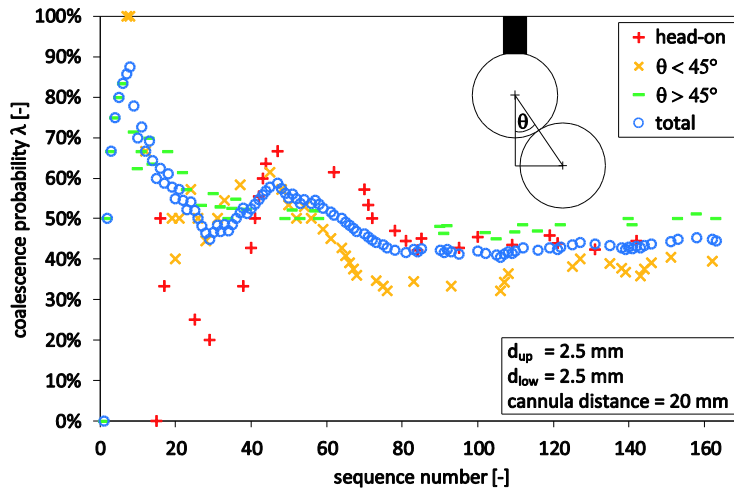


Fig. 5: Trend of coalescence probability over analysed sequences for head-on ($\theta = 0^\circ$), slightly off-centre ($\theta < 45^\circ$) and highly eccentric ($\theta > 45^\circ$) collisions

First investigations using the developed test cell were conducted varying the sizes of the upper and lower droplets between 1.5 and 3.0 mm at a constant cannula distance of 20 mm. In addition, the transfer component acetone was introduced varying the drop sizes and the mass transfer direction. The results are shown in Fig. 6 where the coalescence probability λ is plotted against the equivalent droplet diameter d_{eq} of the colliding droplets. Without mass transfer, the coalescence probability scatters over the range of investigated equivalent drop diameters and no clear trend is identifiable. This seems to be the result of an interference of at least two influencing parameters. With differing size of the lower droplet, the rising velocity changes due to buoyancy. Hence, the two influencing parameters drop size and relative velocity depend on each other and the film drainage model (using a value of $c_1 = 4.375 \cdot 10^{10} \text{ m}^{-4}$) is not able to describe the experimental values by reducing it only to the dependency on the equivalent drop diameter d_{eq} as done in this case. This becomes obvious looking at the three data points with similar equivalent drop size ($d_{eq} = 2.64, 2.69$ and 2.73 mm) in Fig. 6. The two experiments with a bigger droplet at the upper cannula ($d_{low} = 2.5 \text{ mm}$, $d_{up} = 2.8$ and 2.9 mm) result in a coalescence efficiency of 0% and 8%. Whereas the experiment with a bigger droplet rising ($d_{low} = 3.0 \text{ mm}$, $d_{up} = 2.5 \text{ mm}$) shows a coalescence probability of 90%. This shows that the widely used assumption that a collision of drops differing in size but having the same equivalent drop size d_{eq} results in the same coalescence probability is at least exceeded by the influence of the slightly different rising velocity or even questionable. This interference of relative velocity and drop size becomes even more interesting if comparing the implementation of these in existing coalescence models. As shown recently by Kopriwa et. al (2012) the equivalent drop diameter and the energy dissipation rate (from which the relative velocity is commonly calculated) are implemented with different proportionalities and partly even contradictory (Liao and Lucas, 2010). Consequently, the impact of the drop sizes and the rising velocity will be investigated systematically in future analysis. The obtained data will offer an experimental validation and improvement of the modelling approaches. Up to now, the recorded sequences are analysed manually. Evaluating all sequences per parameter set, with about 300 images each, would end up in an analysis of at least 30,000 pictures per data point. Therefore, the velocity of the rising droplet cannot be quantified systematically due to the absence of an automated picture analysis which is developed currently.

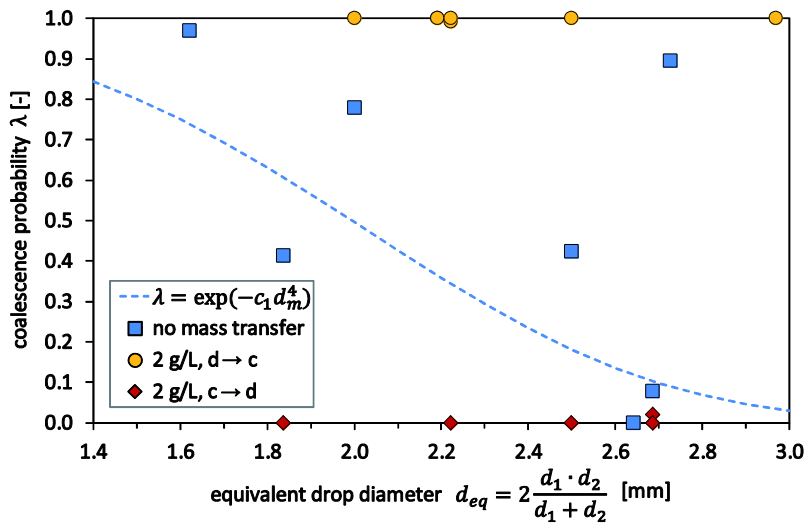


Fig. 6: Influence of equivalent drop diameter and superimposed mass transfer on drop coalescence efficiency at a cannula distance of 20 mm ($1.5 \text{ mm} \leq d_1, d_2 \leq 3.0 \text{ mm}$)

However, the influence of the superimposed mass transfer is enormous. Inducing a mass transfer by a concentration difference of acetone ($\Delta c = 2 \text{ g/L}$) from disperse to continuous phase ($d \rightarrow c$) results in a coalescence probability of about 100%, independent from the drop size and therefore the relative velocity. According to the findings of Chevaillier et al. (2006) and Gourdon and Casamatta (1991), the contact time of the approaching droplets before coalescence occurs is extremely short (within the time span between two recorded images of 1.6 ms) and therefore not measurable with the used high speed camera. Inverting the mass transfer from continuous to disperse phase ($c \rightarrow d$) extends the film drainage time above the overall contact time of the droplets and ends up in a coalescence efficiency about 0%, independent of the drop size and rising velocity as well. The intense influence of the mass transfer can be seen in the supplementary videos of Fig. 7 and 8 showing eight drop collisions in parallel of equal sized droplets with a diameter of 2.5 mm and a concentration difference of $\Delta c = 2 \text{ g/L}$ for both transfer directions.

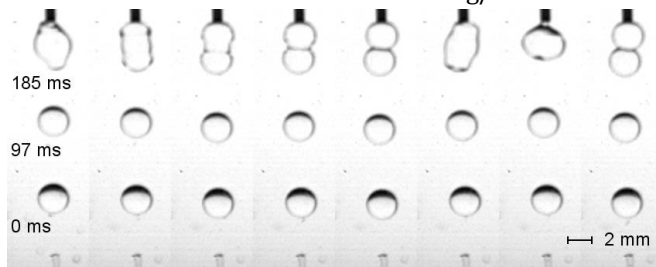


Fig. 7: Video of eight sequences in parallel of equally sized droplets ($d_{up} = 2.5 \text{ mm}$, $d_{low} = 2.5 \text{ mm}$, mass transfer $d \rightarrow c$ with $\Delta c = 2 \text{ g/L}$, cannula distance = 20 mm, 150 frames recorded with 620 fps)

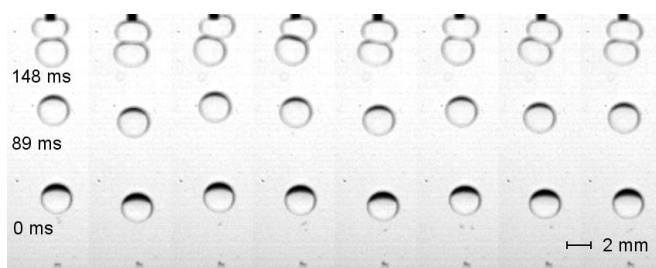


Fig. 8: Video of eight sequences in parallel of equally sized droplets ($d_{up} = 2.5 \text{ mm}$, $d_{low} = 2.5 \text{ mm}$, mass transfer $c \rightarrow d$ with $\Delta c = 2 \text{ g/L}$, cannula distance = 20 mm, 150 frames recorded with 620 fps)

Conclusions

By using the novel test cell for single drop coalescence analysis, it is possible to conduct a serial examination of the coalescence probability varying particular parameters. A good observability due to a combination of static and dynamic droplet collision, a high repetition rate of 2 - 3 recorded sequences per minute and a good reproducibility of the collisions enable an examination of at least 100 collisions per parameter set, which is important for statistical analysis. The influence of drop size ratio seems to be interfered by the different relative velocities of the droplets, hence a clear trend could not be found and will be the objective of further investigations. To determine the relative velocity for each sequence, an automated picture analysis is required and developed currently. This will also allow the quantification of contact and coalescence time, droplet deformation and coalescence probability. Superimposed mass transfer influences the coalescence significantly: mass transfer from disperse to continuous phase results in a coalescence of nearly all droplets and inverting the mass transfer direction retards the coalescence almost completely.

Acknowledgements

The authors kindly thank the student workers Michael Meinke and Koray Yesilli who substantially contributed to this work. Financial support provided by the German Research Foundation (DFG) within the project KR 1639/19-1 is gratefully acknowledged.

Literature

- Aarts, D.G.A.L., Lekkerkerker, H.N.W., Guo, H., Wegdam, G.H., Bonn, D., 2005. Hydrodynamics of droplet coalescence. *Phys. Rev. Lett.* 95, 164503, DOI: 10.1103/PhysRevLett.95.164503
- Abid, S., Chesters, A.K., 1994. The drainage and rupture of partially-mobile films between colliding drops at constant approach velocity. *Int. J. Multiphase Flow* 20, 613–629, DOI: 10.1016/0301-9322(94)90033-7
- Aryafar, H., Kavehpour, H.P., 2006. Drop coalescence through planar surfaces. *Phys. Fluids* 18, 72105, DOI: 10.1063/1.2227435
- Baldessari, F., Leal, L.G., 2006. Effect of overall drop deformation on flow-induced coalescence at low capillary numbers. *Phys. Fluids* 18, 13602, DOI: 10.1063/1.2158427
- Ban, T., Kawaizumi, F., Nii, S., Takahashi, K., 2000. Study of drop coalescence behavior for liquid-liquid extraction operation. *Chem. Eng. Sci.* 55, 5385–5391, DOI: 10.1016/S0009-2509(00)00156-1
- Basheva, E.S., Gurkov, T.D., Ivanov, I.B., Bantchev, G.B., Campbell, B., Borwankar, R.P., 1999. Size dependence of the stability of emulsion drops pressed against a large interface. *Langmuir* 15, 6764–6769, DOI: 10.1021/la990186j
- Borrell, M., Leal, L.G., 2008. Viscous coalescence of expanding low-viscosity drops; the dueling drops experiment. *J. Colloid Interface Sci.* 319, 263–269, DOI: 10.1016/j.jcis.2007.11.041
- Borrell, M., Yoon, Y., Leal, L.G., 2004. Experimental analysis of the coalescence process via head-on collisions in a time-dependent flow. *Phys. Fluids* 16, 3945–3954, DOI: 10.1063/1.1795291
- Bozzano, G., Dente, M., 2011. Modelling the drop coalescence at the interface of two liquids. *Comput. Chem. Eng.* 35, 901–906, DOI: <http://dx.doi.org/10.1016/j.compchemeng.2011.01.022>
- Carroll, B.J., 1976. The stability of emulsions and mechanisms of emulsion breakdown, in: Matijevic, E. (Ed.), *Surface and Colloid Science*, Vol. 9. Wiley-Interscience, New York, pp. 1–68

- Charles, G.E., Mason, S.G., 1960. The mechanism of partial coalescence of liquid drops at liquid/liquid interfaces. *J. Colloid Sci.* 15, 105–122, DOI: 10.1016/0095-8522(60)90012-X
- Chen, D., Pu, B., 2001. Studies on the binary coalescence model: II. Effects of drops size and interfacial tension on binary coalescence time. *J. Colloid Interface Sci.* 243, 433–443, DOI: 10.1006/jcis.2001.7817
- Chen, J.-D., 1985. A model of coalescence between two equal-sized spherical drops or bubbles. *J. Colloid Interface Sci.* 107, 209–220, DOI: 10.1016/0021-9797(85)90164-X
- Chen, N., Kuhl, T., Tadmor, R., Lin, Q., Israelachvili, J., 2004. Large deformations during the coalescence of fluid interfaces. *Phys. Rev. Lett.* 92, 24501, DOI: 10.1103/PhysRevLett.92.024501
- Chesters, A.K., 1991. The modeling of coalescence processes in fluid-liquid dispersions: a review of current understanding. *Chem. Eng. Res. Des.* 69, 259–270
- Chevallier, J.P., Klaseboer, E., Masbernat, O., Gourdon, C., 2006. Effect of mass transfer on the film drainage between colliding drops. *J. Colloid Interface Sci.* 299, 472–485, DOI: 10.1016/j.jcis.2006.02.005
- Coulaloglou, C.A., Tavlarides, L.L., 1977. Description of interaction processes in agitated liquid-liquid dispersions. *Chem. Eng. Sci.* 32, 1289–1297, DOI: 10.1016/0009-2509(77)85023-9
- Danov, K.D., Petsev, D.N., Denkov, N.D., Borwankar, R., 1993. Pair interaction energy between deformable drops and bubbles. *J. Chem. Phys.* 99, 7179, DOI: 10.1063/1.465434
- Dickinson, E., Murray, B.S., Stainsby, G., 1988. Coalescence stability of emulsion-sized droplets at a planar oil-water interface and the relationship to protein film surface rheology. *J. Chem. Soc., Faraday Trans. 1* 84, 871, DOI: 10.1039/f19888400871
- Eckstein, A., Vogelpohl, A., 1999. Untersuchungen zur Tropfen-Tropfen-Koaleszenz. *Chem. Ing. Tech.* 71, 480–483, DOI: 10.1002/cite.330710512
- Eggers, J., Lister, J.R., Stone, H.A., 1999. Coalescence of liquid drops. *J. Fluid Mech.* 401, 293–310, DOI: 10.1017/S002211209900662X
- Eiswirth, R.T., Bart, H.-J., Ganguli, A.A., Kenig, E.Y., 2012. Experimental and numerical investigation of binary coalescence: Liquid bridge building and internal flow fields. *Phys. Fluids* 24, 62108, DOI: 10.1063/1.4729791
- Gaitzsch, F., Gäbler, A., Kraume, M., 2011a. Analysis of droplet expulsion in stagnant single water-in-oil-in-water double emulsion globules. *Chem. Eng. Sci.* 66, 4663–4669, DOI: 10.1016/j.ces.2011.06.020
- Gaitzsch, F., Kamp, J., Kraume, M., Gäbler, A., 2011b. Vergleich des Koaleszenzverhaltens ruhender und umströmter Wasser-in-Öl-in-Wasser-Einzeltropfen. *Chem. Ing. Tech.* 83, 511–517, DOI: 10.1002/cite.201100006
- Gourdon, C., Casamatta, G., 1991. Influence of mass-transfer direction on the operation of a pulsed sieve-plate pilot column. *Chem. Eng. Sci.* 46, 2799–2808, DOI: 10.1016/0009-2509(91)85149-R
- Guido, S., Simeone, M., 1998. Binary collision of drops in simple shear flow. *J. Fluid Mech.* 357, 1–20, DOI: 10.1017/S0022112097007921

- Hartland, S., 1967a. The coalescence of a liquid drop at a liquid-liquid interface Part I: Drop shape. *Trans. Instn. Chem. Engrs.* 45, T97-101
- Hartland, S., 1967b. The coalescence of a liquid drop at a liquid-liquid interface Part II: Film thickness. *Trans. Instn. Chem. Engrs.* 45, T102-108
- Hartland, S., 1967c. The coalescence of a liquid drop at a liquid-liquid interface Part III: Film rupture. *Trans. Instn. Chem. Engrs.* 45, T109-114
- Hool, K.O., Saunders, R.C., Ploehn, H.J., 1998. Measurement of thin liquid film drainage using a novel high-speed impedance analyzer. *Rev. Sci. Instrum.* 69, 3232-3239, DOI: 10.1063/1.1149088
- Hulburt, H.M., Katz, S., 1964. Some problems in particle technology. *Chem. Eng. Sci.* 19, 555-574, DOI: 10.1016/0009-2509(64)85047-8
- Ivanov, I.B., Danov, K.D., Kralchevsky, P.A., 1999. Flocculation and coalescence of micron-size emulsion droplets. *Colloids Surf., A* 152, 161-182, DOI: 10.1016/S0927-7757(98)00620-7
- Jeffreys, G. V, Hawksley, J.L., 1965. Coalescence of liquid droplets in two-component-two-phase systems: Part II. Theoretical analysis of coalescence rate. *AIChE J.* 11, 418-424, DOI: 10.1002/aic.690110310
- Klaseboer, E., Chevaillier, J.P., Gourdon, C., Masbernat, O., 2000. Film drainage between colliding drops at constant approach velocity: experiments and modeling. *J. Colloid Interface Sci.* 229, 274-285, DOI: 10.1006/jcis.2000.6987
- Kopriwa, N., Buchbender, F., Ayesteran, J., Kalem, M., Pfennig, A., 2012. A Critical Review of the Application of Drop-Population Balances for the Design of Solvent Extraction Columns: I. Concept of Solving Drop-Population Balances and Modelling Breakage and Coalescence. *Solvent Extr. Ion Exch.* 30, 683-723, DOI: 10.1080/07366299.2012.700598
- Kourio, M.J., Gourdon, C., Casamatta, G., 1994. Study of drop-interface coalescence: Drainage time measurement. *Chem. Eng. Technol.* 17, 249-254, DOI: 10.1002/ceat.270170406
- Kumar, M.K., Mitra, T., Ghosh, P., 2006. Adsorption of ionic surfactants at liquid-liquid interfaces in the presence of salt: Application in binary coalescence of drops. *Ind. Eng. Chem. Res.* 45, 7135-7143, DOI: 10.1021/ie0604066
- Leal, L.G., 2004. Flow induced coalescence of drops in a viscous fluid. *Phys. Fluids* 16, 1833, DOI: 10.1063/1.1701892
- Lee, J.C., Hodgson, T.D., 1968. Film flow and coalescence. I. Basic relations, film shape, and criteria for interface mobility. *Chem. Eng. Sci.* 23, 1375-1397, DOI: 10.1016/0009-2509(68)89047-5
- Liao, Y., Lucas, D., 2009. A literature review of theoretical models for drop and bubble breakup in turbulent dispersions. *Chem. Eng. Sci.* 64, 3389-3406, DOI: 10.1016/j.ces.2009.04.026
- Liao, Y., Lucas, D., 2010. A literature review on mechanisms and models for the coalescence process of fluid particles. *Chem. Eng. Sci.* 65, 2851-2864, DOI: 10.1016/j.ces.2010.02.020
- Mackay, G.D.M., Mason, S.G., 1963. The gravity approach and coalescence of fluid drops at liquid interfaces. *Can. J. Chem. Eng.* 41, 203-212, DOI: 10.1002/cjce.5450410504
- Marrucci, G., 1969. A theory of coalescence. *Chem. Eng. Sci.* 24, 975-985, DOI: 10.1016/0009-2509(69)87006-5

- Misek, T., Berger, R., Schröter, J., 1985. Standard test systems for liquid extraction, 2nd Ed. ed. The Institution of Chemical Engineers, Rugby, UK
- Mohamed-Kassim, Z., Longmire, E.K., 2004. Drop coalescence through a liquid/liquid interface. *Phys. Fluids* 16, 2170, DOI: 10.1063/1.1735686
- Neumann, H.J., 1963. Beitrag zum Mechanismus der Koaleszenz. *Naturwissenschaften* 50, 544–545, DOI: 10.1007/BF00623577
- Ortiz-Duenas, C., Kim, J., Longmire, E.K., 2010. Investigation of liquid-liquid drop coalescence using tomographic PIV. *Exp. Fluids* 49, 111–129, DOI: 10.1007/s00348-009-0810-7
- Pu, B., Chen, D., 2001. Studies on the binary coalescence model: I. Jumping coalescence phenomenon. *J. Colloid Interface Sci.* 235, 1–3, DOI: DOI: 10.1006/jcis.2000.7305
- Radoev, B., Scheludko, A., Manev, E., 1983. Critical thickness of thin liquid films: theory and experiment. *J. Colloid Interface Sci.* 95, 254–265, DOI: 10.1016/0021-9797(83)90094-2
- Ramkrishna, D., 1985. Status of population balances. *Rev. Chem. Eng.* 3, 49–95, DOI: 10.1515/REVCE.1985.3.1.49
- Ramkrishna, D., 2000. Population Balances: Theory and Applications to Particulate Systems in Engineering. Academic Press, San Diego
- Randolph, A.D., Larson, M.A., 1962. Transient and steady state size distributions in continuous mixed suspension crystallizers. *AIChE J.* 8, 639–645, DOI: 10.1002/aic.690080515
- Sagert, N.H., Quinn, M.J., 1978. The coalescence of n-Hexane droplets in aqueous electrolyte solutions. *Can. J. Chem. Eng.* 56, 679–684, DOI: 10.1002/cjce.5450560605
- Scheele, G.F., Leng, D.E., 1971. An experimental study of factors which promote coalescence of two colliding drops suspended in water - I. *Chem. Eng. Sci.* 26, 1867–1879, DOI: 10.1016/0009-2509(71)86030-X
- Scheludko, A., Platikanov, D., Manev, E., 1965. Disjoining pressure in thin liquid films and the electro-magnetic retardation effect of the molecule dispersion interactions. *Discuss. Faraday Soc.* 40, 253–265, DOI: 10.1039/DF9654000253
- Simon, M., Bart, H.-J., 2002. Experimental studies of coalescence in liquid-liquid systems. *Chem. Eng. Technol.* 25, 481–484, DOI: 10.1002/1521-4125(200205)25:5<481::AID-CEAT481>3.0.CO;2-T
- Soika, M., Pfennig, A., 2005. Extraktion - Eine Frage des Wassers? *Chem. Ing. Tech.* 77, 905–911, DOI: 10.1002/cite.200500032
- Thoroddsen, S.T., 2006. Fluid dynamics: Droplet genealogy. *Nat. Phys.* 2, 223–224, DOI: 10.1038/nphys276
- Thoroddsen, S.T., Takehara, K., Etoh, T.G., 2005. The coalescence speed of a pendent and a sessile drop. *J. Fluid Mech.* 527, 85–114, DOI: 10.1017/S0022112004003076
- Toro-Mendoza, J., Petsev, D.N., 2010. Brownian dynamics of emulsion film formation and droplet coalescence. *Phys. Rev. E: Stat., Nonlinear, Soft Matter Phys.* 81, 51404, DOI: 10.1103/PhysRevE.81.051404

- Tsouris, C., Tavlarides, L.L., 1993. Mass-transfer effects on droplet phenomena and extraction column hydrodynamics revisited. *Chem. Eng. Sci.* 48, 1503–1515, DOI: 10.1016/0009-2509(93)80055-U
- Vijayan, S., Ponter, A.B., 1975. Drop/drop and drop/interface coalescence in primary liquid/liquid dispersion separators. *Chem. Ing. Tech.* 47, 748–755, DOI: 10.1002/cite.330471803
- Vohra, D.K., Hartland, S., 1981. Effect of geometrical arrangement and interdrop forces on coalescence time. *Can. J. Chem. Eng.* 59, 438–449, DOI: 10.1002/cjce.5450590405
- Vrij, A., 1966. Possible mechanism for the spontaneous rupture of thin, free liquid films. *Discuss. Faraday Soc.* 42, 23–33, DOI: 10.1039/DF9664200023
- Wegener, M., Fevre, M., Paschedag, A.R., Kraume, M., 2009. Impact of Marangoni instabilities on the fluid dynamic behaviour of organic droplets. *Int. J. Heat Mass Transfer* 52, 2543–2551, DOI: 10.1016/j.ijheatmasstransfer.2008.11.022
- Wu, M., Cubaud, T., Ho, C.-M., 2004. Scaling law in liquid drop coalescence driven by surface tension. *Phys. Fluids* 16, L51–L54, DOI: 10.1063/1.1756928
- Yang, H., Park, C.C., Hu, Y.T., Leal, L.G., 2001. The coalescence of two equal-sized drops in a two-dimensional linear flow. *Phys. Fluids* 13, 1087–1106, DOI: 10.1063/1.1358873
- Zdravkov, A.N., Peters, G.W.M., Meijer, H.E.H., 2003. Film drainage between two captive drops: PEO-water in silicon oil. *J. Colloid Interface Sci.* 266, 195–201, DOI: 10.1016/S0021-9797(03)00466-1
- Zdravkov, A.N., Peters, G.W.M., Meijer, H.E.H., 2006. Film drainage and interfacial instabilities in polymeric systems with diffuse interfaces. *J. Colloid Interface Sci.* 296, 86–94, DOI: 10.1016/j.jcis.2005.08.062